2021 43rd Annual International Conference of the
IEEE Engineering in Medicine & Biology Society (EMBC)
Oct 31 - Nov 4, 2021. Virtual Conference

Sources and Sinks in Interictal iEEG Networks: An iEEG Marker of the Epileptogenic Zone

Kristin M. Gunnarsdottir[1], Jorge Gonzalez-Martinez[2], Simon Wing[1] and Sridevi V. Sarma[1]

Abstract— **Around 30% of epilepsy patients have seizures that cannot be controlled with medication. The most effective treatments for medically resistant epilepsy are interventions that surgically remove the epileptogenic zone (EZ), the regions of the brain that initiate seizure activity. A precise identification of the EZ is essential for surgical success but unfortunately, current success rates range from 20-80%. Localization of the EZ requires visual inspection of intracranial EEG (iEEG) recordings during seizure events. The need for seizure occurrence makes the process both costly and time-consuming and in the end, less than 1% of the data captured is used to assist in EZ localization. In this study, we aim to leverage interictal (between seizures) data to localize the EZ. We develop and test the source-sink index as an interictal iEEG marker by identifying two groups of network nodes from a patient's interictal iEEG network: those that inhibit a set of their neighboring nodes ("sources") and the inhibited nodes themselves ("sinks"). Specifically, we i) estimate patient-specific dynamical network models from interictal iEEG data and ii) compute a source-sink index for every network node (iEEG channel) to identify pathological nodes that correspond to the EZ. Our results suggest that in patients with successful surgical outcomes, the source-sink index clearly separates the clinically identified EZ (CA-EZ) channels from other channels whereas in patients with failed outcomes CA-EZ channels cannot be distinguished from the rest of the network.**

I. INTRODUCTION

Epilepsy is a chronic neurological disorder characterized by unprovoked, recurrent seizures. Although about 70% of patients diagnosed with epilepsy respond positively to medication, 30% have seizures that cannot be controlled with drugs [1]. The most effective treatment for medically resistant epilepsy (MRE) is surgical removal or disconnection of the epileptogenic zone (EZ), the region, or network of regions, of the brain that initiate seizure activity [2]. A precise identification of the EZ is essential for surgical success, but unfortunately current success rates vary, ranging from 20-80% [3].

Before the surgery, patients undergo a thorough evaluation process to determine the location of the EZ. When non-invasive methods (e.g. electroencephalography (EEG) and neuroimaging modalities) are inconclusive in localizing the EZ, invasive monitoring with intracranial EEG (iEEG) is often needed. Then, the patient remains in the hospital for several days to weeks waiting for a sufficient number of seizure (ictal) events because the current clinical standard entails analyzing multiple of these events, looking for abnormal epileptic signatures, in order to localize the EZ. The iEEG channels that show the earliest signs of these signatures are generally identified as the EZ. Although clinicians also inspect interictal (between seizures) data to look for epileptic activity such as interictal discharges, these discharges have not been proven to be reliable iEEG markers of the EZ and thus the gold standard predominantly relies on inspecting seizure events. As such, more than 99% of the iEEG recordings captured invasively from patients are ignored.

In recent years, epilepsy has been increasingly conceptualized as a network disorder rather than a single source of pathology in the human brain [4]–[6]. Intracranial EEG offers a unique opportunity to observe rich epileptic cortical network dynamics, which are only visible to the naked eye during seizures. However, the need for seizure occurrence makes localization of the EZ a costly and time-consuming process and poses an increased risk to patients [7]. The process is also subjective, as no iEEG markers are used by clinicians to specifically assist in identifying the EZ.

In this study, we aim to leverage data captured between seizures to localize the EZ. We hypothesize that when a patient is not having a seizure, it is because the EZ is being inhibited by neighboring regions. We thus will develop and test a new interictal iEEG marker of the EZ by identifying two groups of nodes from a patient's interictal iEEG network: those that are continuously inhibiting a set of their neighboring nodes (denoted as "sources") and the inhibited nodes themselves (denoted as "sinks"). Specifically, we will develop a computational tool that i) estimates patient-specific dynamical network models from interictal iEEG data and ii) uses source-sink connectivity properties of the models to identify pathological nodes (iEEG channels) in the network that correspond to the EZ. We apply our algorithm to interictal iEEG data from 6 patients and evaluate performance by comparing the EZ channels identified by our algorithm to those identified by clinicians.

II. METHODS

A. iEEG Dataset

The data analyzed in this study were stereotactic EEG (SEEG) recordings from six patients treated at the Cleveland Clinic. All patients have focal MRE and underwent robotic stereotactic placement of depth electrodes for extra-operative monitoring followed by laser ablation. Successful surgical outcomes were defined as seizure free (Engel class I [8])) and failure outcomes as seizure recurrence (Engel classes II-IV) at 12+ months post-operation. Three patients had

[1]K. M. Gunnarsdottir, S. Wing and S. V. Sarma are with Johns Hopkins University, Baltimore, MD, USA kgunnar1@jhu.edu

[2]J. Gonzalez-Martinez is with University of Pittsburgh Medical Center, PA, USA

successful outcomes and three had failed outcomes. For each patient, the clinical team identified the iEEG channels they hypothesized as EZ (CA-EZ). The data were recorded using the Nihon Kohden diagnostic and monitoring system (Nihon Kohden America, Foothill Ranch, CA, USA) at a sampling frequency of 1 kHz. For each patient, we analyzed one interictal snapshot (typically recorded hours before seizure events) and one seizure snapshot that consisted of the seizure event as well as a few minutes before and after seizure. All data were acquired with approval of the Cleveland Clinic Institutional Review Board. More details about the dataset are presented in Table I.

B. Data Preprocessing

The data were bandpass filtered between 0.5 and 300 Hz with a fourth order Butterworth filter, and notch filtered at 60 Hz. A common average reference was applied to remove common noise from the signals. All iEEG channels not recording from grey matter or otherwise deemed "bad" (e.g., broken or excessively noisy) by visual inspection were discarded from each patient's dataset.

C. Dynamical Network Models

The dynamical network models (DNMs) are generative models that characterize how each iEEG channel dynamically interacts with the rest of the network. The interictal DNM took the form of a linear time-varying (LTV) model which was constructed by forming a sequence of linear time-invariant (LTI) DNMs derived for each 500 msec window of the data. Each LTI model was defined as:

$$\boldsymbol{x}(t+1) = \boldsymbol{A}_w \boldsymbol{x}(t) \quad (1)$$

where $\boldsymbol{x}(t) \varepsilon \mathbb{R}^{Nx1}$ is the state vector and represents the implanted iEEG channels, $\boldsymbol{A}_w \varepsilon \mathbb{R}^{NxN}$ is the state transition matrix computed from window w and N is the number of iEEG channels. In our previous work, we showed how DNMs can be derived using least squares estimation and that they accurately reconstruct iEEG time series [9].

D. Source-Sink Hypothesis

We defined two special types of nodes in the iEEG network. A node is a "*source*" if it has a high influence on other nodes in the network but is not highly influenced by the rest of the network, and a "*sink*" if it is highly influenced by the activity of other nodes, but does not have a high influence on others. This is reflected by the rows and columns of $\boldsymbol{A}_w$. Sources are channels that have high values in their columns but low values across their rows, whereas sinks have high row values and low column values.

An epilepsy patient has a seizure when the EZ is triggered, and the EZ nodes work together to initiate and spread the seizure activity to neighboring regions. On the other hand, seizures are suppressed when the EZ is effectively inhibited by its neighboring regions. In terms of sources and sinks, we hypothesized that EZ nodes are *sources* right before a seizure but become *sinks* at rest. From a pathological standpoint, the source-sink hypothesis is supported by clinical evidence based on elevated levels of glutamate and glutamate transporters in patients with epilepsy [10], [11]. A recent iEEG study also provided further evidence by demonstrating a high inward-directed connectivity to the EZ from resting state fMRI [12].

TABLE I

PATIENT DEMOGRAPHICS.

	Number of Patients	Sex (M/F)	Surgery Age (Years)	MRI (NL/ABN)	Number of Contacts
Success	3	2/1	28 ± 13	2/1	67 ± 21
Failure	3	2/1	31 ± 12	2/1	110 ± 30

NL = MRI normal, ABN = Abnormal findings on MRI.

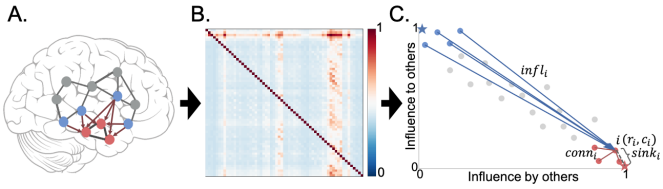

Fig. 1. A. N-channel iEEG network example. B. Corresponding $\boldsymbol{A}$ matrix in window w. C. 2D source-sink representation of the network with sink index ($sink_i$), source influence ($infl_i$) and sink connectivity ($conn_i$) labeled.

Although iEEG provide a much more direct measure of local neuronal population activity compared to traditional EEG, each iEEG channel records the activity of about half a million neurons [13]. Consequently, the DNMs cannot distinguish between excitatory and inhibitory connections in the iEEG network. Thus, we only quantified the strength of the connection between two nodes, hereafter referred to as the amount of "influence" one node has on another.

E. Source-Sink Analysis

For each patient, the DNMs were estimated in non-overlapping 500 msec windows of the iEEG data to obtain a sequence of $\boldsymbol{A}$ matrices over time, $\boldsymbol{A}_w$, $w \varepsilon [1,2,..,T]$, where T is the number of 500 msec windows. In each $\boldsymbol{A}_w$ (Fig. 1B), row i represents the amount of influence the rest of the network has on channel i in window w, and column j represents how the activity of channel j influences the rest of the network.

1) Identifying Top Sources and Sinks: Next, we identified the top sources and sinks from $\boldsymbol{A}_w$. The extent of each channel's source/sink behavior can be quantified by computing the total influence to and from each channel, defined as the sums of the columns and rows of $abs(\boldsymbol{A}_w)$, ranked against each other (rank 1/N indicates smallest sum, rank 1 is largest sum). When drawn in the source-sink 2D space (Fig. 1C), sources are channels located at the top left, whereas sinks are located at the bottom right.

2) Computing Source-Sink Indices: Once the top sources and sinks were identified, we computed a source-sink index, *ss*, for each channel to find the channels in the hypothesized source-sink EZ (SS-EZ). The source-sink index is the product of three metrics subject to the source-sink hypothesis. For each channel i, in each window w, we quantified the following metrics:

Sink Index: The first criterion for EZ nodes is being a top sink. The sink index captures how close a node is to the ideal sink, which is defined as a node whose row rank is 1 and column rank is 0 (see Fig. 1C, pink star). The sink index was computed as:

$$sink_i^w = \sqrt{2} - ||(r_i, c_i) - (1,0)|| \quad (2)$$

where r_i and c_i are the row and column ranks of channel i, respectively. The larger the sink index, the more likely the channel is a sink.

Source Index: Similar to the sink index, the source index captures how close a channel is to the ideal source (blue star in Fig. 1C):

$$source_i^w = \sqrt{2} - ||(r_i, c_i) - (0,1)|| \quad (3)$$

Source Influence: The second criterion requires EZ nodes to be highly influenced by top sources. The source influence score quantifies how much the top sources influence channel i and was defined as:

$$infl_i^w = \sum_{j=1}^{N} A_{ij} * source_j \quad (4)$$

Sink Connectivity: The third EZ criterion is high connectivity to other sinks. The sink connectivity index quantifies the strength of connections from the top sinks to channel i:

$$conn_i^w = \sum_{j=1}^{N} A_{ij} * sink_j \quad (5)$$

All metrics are normalized by maximum value.

Source-Sink Index: Finally, a source-sink activation index was computed for each iEEG channel as:

$$ss_i^w = sink_i * infl_i * conn_i \quad (6)$$

In line with the source-sink hypothesis, ss_i^w is high if all three indices are high. Therefore, we expected EZ nodes to have a high source-sink index, but non-EZ nodes to have a lower index, in patients with successful surgical outcomes.

III. RESULTS

1) Identifying Hypothesized Source-Sink EZ (SS-EZ): We defined the top sources/sinks in the iEEG network for each patient as the 10% of channels exhibiting the strongest source/sink behavior at rest (interictally). See Fig. 2B and F for examples of the 2D source-sink space for one success and one failure patient, respectively. In patients with successful surgical outcomes, the CA-EZ channels are expected to be a subset of the top sinks (Fig. 2B). Pink/blue arrows indicate the strongest connections from each top source/sink and the channels they point to. SS-EZ channels were defined as the subset of sinks that at least one source and one sink connect to. In general, the top sources and sinks point to the SS-EZ channels in success patients (Fig. 2B), whereas they may also connect to other channels in patients with failed surgical outcomes (Fig. 2F).

2) Computing Source-Sink Indices: For each patient, we computed each channel's source-sink index (eq. (6)) in 500 msec windows of one interictal and one seizure snapshot (Fig. 2C and G). Note that the two snapshots are not consecutive in time as the interictal snapshot is typically recorded hours before the seizure event. As Fig. 2C shows, the CA-EZ channels (3 out of 3) are top sinks in the iEEG network and the patient had a successful surgical outcome. At

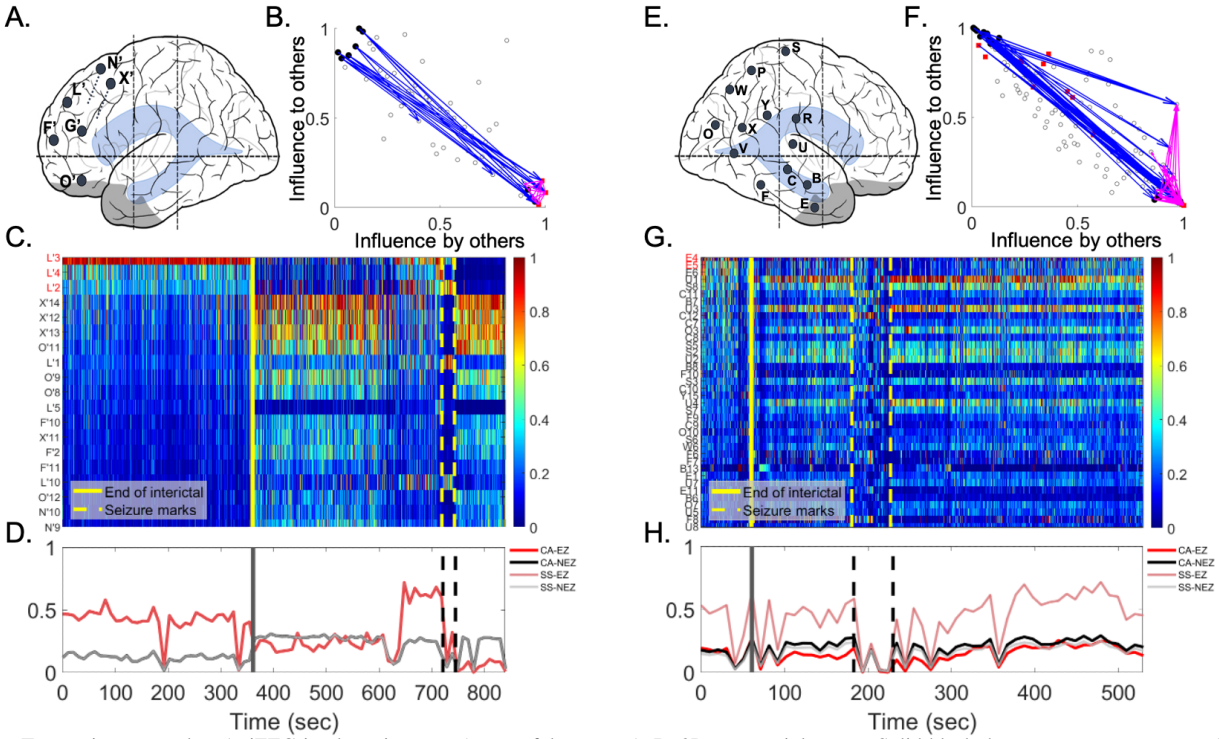

Fig. 2. Two patient examples. A. iEEG implantation map (successful outcome). B. 2D source-sink space. Solid black dots represent top sources (top left) and sinks (bottom right) and red squares represent the CA-EZ. The most influential connections from sources (blue arrows) point to the sinks. Strongest connections from sinks (pink arrows) point to other sinks. C. Source-sink index of every channel during interictal (left) and ictal (right) periods, separated by the solid yellow line. Channels are arranged from highest to lowest average interictal ss_i. CA-EZ channels are colored red. Only the top 30% of channels are shown for better visualization purposes, and all channels not shown have low ss_i^w values. D. Average source-sink index of four groups of channels: CA-EZ, CA-NEZ, SS-EZ and SS-NEZ. In this success patient there is perfect agreement between the CA-EZ and SS-EZ. E. iEEG implantation map (failure outcome). F. 2D source-sink space. In this failure patient, top sources point to nodes other than top sinks. Top sinks also point to these other nodes. G. Source-sink index of every channel over time. Only 2 out of 13 CA-EZ channels have a high source-sink index. H. Average source-sink index of the four groups. In this failure patient CA-EZ cannot be distinguished from CA-NEZ.

rest these channels (in particular L'3) have a high source-sink index, suggesting that they are top sinks strongly influenced by the top sources. However, during and right after seizure, the same channels have a low index, i.e. they are exhibiting a strong source-like behavior. In contrast, only a small subset (2 out of 13) of CA-EZ channels are amongst the top sinks in a patient with a failed surgical outcome (Fig. 2G).

The temporal source-sink index modulation is summarized in Fig. 2D and H. We computed the average *ss* for four groups of interest: i) CA-EZ channels, ii) all other channels not labeled as CA-EZ (CA-NEZ), iii) SS-EZ, and iv) all other channels not labeled as SS-EZ (SS-NEZ). Note that the sets are not disjoint, i.e. groups iii) and iv) are comprised of channels from i) and/or ii). Each curve was obtained by computing the average *ss* of each channel group, in each window. The curves were smoothed by computing the index across 10 second windows instead of 500 msec. As Fig. 2D shows, the CA-EZ channels follow a very similar temporal modulation pattern as the SS-EZ, and have a higher *ss* than the rest of the network. However, this does not hold true for the failure patient (Fig. 2H), where the mean *ss* of the CA-EZ is much lower than that of the SS-EZ at rest. Moreover, it is slightly lower than the mean index of the rest of the channels in the network.

Finally, Fig. 3 compares the temporal source-sink index modulation in success versus failure patients. For each patient, *ss* was computed in four predefined windows: a) a 30 second window of the interictal recording, b) 60-30 seconds before the seizure event, c) during the seizure event, and d) 60-90 seconds after the end of seizure. For each set of channels, indices were normalized to the average *ss* of the entire network at rest (window a). At each time point, we then computed the mean $\pm$ standard deviation of *ss* across the three success patients (top) and the three failure patients (bottom). In the success patients, the CA-EZ and the SS-EZ demonstrate the same dynamic trends and have a higher source-sink index compared to the rest of the channels in the network. The same cannot be said about the failure patients, as the CA-EZ channels have a much lower *ss* compared to the SS-EZ and are not separable from the CA-NEZ channels. Note however, that the SS-EZ and SS-NEZ curves follow very similar dynamics in both groups of patients.

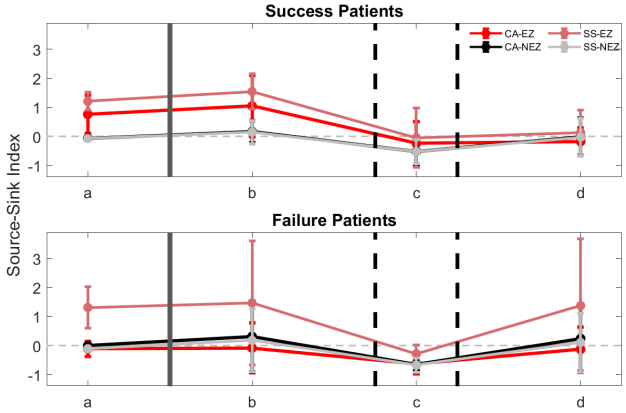

Fig. 3. Temporal modulation of the source-sink index in success versus failure patients. Average *ss* of four groups of channels: CA-EZ, CA-NEZ, SS-EZ and SS-NEZ. Each curve shows the mean $\pm$ std across 3 success patients (top) and 3 failure patients (bottom).

IV. DISCUSSION

In this study, we tested the source-sink index as an interictal iEEG marker of the EZ. We computed the source-sink index for all implanted iEEG channels and examined its properties at rest and during seizures. In patients with successful surgical outcomes, the magnitude and dynamics of *ss* across the SS-EZ channels highly correlated with the CA-EZ, and clearly separated these channels from the rest of the network. In patients with failure outcomes however, there was little to no *ss* modulation of CA-EZ and CA-NEZ channels and these groups could not be distinguished from one another.

Future work involves testing and validating the source-sink algorithm on a larger set of patients as well as further quantifying the source-sink modulation as the brain transitions from an interictal to an ictal state. Although preliminary, our results suggest that the source-sink index, a metric entirely based on the properties of the iEEG network at rest, captures the characteristics of the regions responsible for seizure initiation and may be a promising marker of the EZ.

REFERENCES

[1] P. Kwan and J. Sander, "The natural history of epilepsy: an epidemiological view," *J Neurol Neurosurg Psychiatry*, vol. 75, pp. 1376–1381, 2004.

[2] H. O. Lüders, I. Najm, D. Nair, and et al, "The epileptogenic zone: general principles," *Epileptic Disord*, vol. 8, pp. S1–9, 2006.

[3] W. L. Ramey, N. L. Martirosyan, C. M. Lieu, and et al, "Current management and surgical outcomes of medically intractable epilepsy," *Clinical Neurology and Neurosurgery*, vol. 115, no. 12, pp. 2411–2418, 2013.

[4] W. Stacey, M. Kramer, K. Gunnarsdottir, and et al, "Emerging roles of network analysis for epilepsy," *Epilepsy Research*, vol. 159, 2020.

[5] A. Li, B. Chennuri, S. Subramanian, and et al, "Using network analysis to localize the epileptogenic zone from invasive eeg recordings in intractable focal epilepsy," *Network Neuroscience*, vol. 02, pp. 218–240, 06 2018.

[6] S. P. Burns, S. Santaniello, R. B. Yaffe, C. C. Jouny, N. E. Crone, G. K. Bergey, W. S. Anderson, and S. V. Sarma, "Network dynamics of the brain and influence of the epileptic seizure onset zone," *Proceedings of the National Academy of Sciences*, vol. 111, no. 49, pp. E5321–E5330, 2014.

[7] D. R. Nair, R. Burgess, C. C. McIntyre, and H. Lüders, "Chronic subdural electrodes in the management of epilepsy," *Clinical Neurophysiology*, vol. 119, no. 1, pp. 11–28, 2008.

[8] J. Engel Jr., "Outcome with respect to epileptic seizures," *Surg. Treat. Epilepsies*, pp. 609–621, 1993.

[9] A. Li, K. M. Gunnarsdottir, S. Inati, and et al, "Linear time-varying model characterizes invasive EEG signals generated from complex epileptic networks," in *2017 39th Annual International Conference of the IEEE Engineering in Medicine and Biology Society (EMBC)*, pp. 2802–2805, 2017.

[10] M. During and D. Spencer, "Extracellular hippocampal glutamate and spontaneous seizure in the conscious human brain," *The Lancet*, vol. 341, no. 8861, pp. 1607–1610, 1993.

[11] P. B. Crino, H. Jin, M. . Shumate, and et al, "Increased expression of the neuronal glutamate transporter (eaat3/eaac1) in hippocampal and neocortical epilepsy," *Epilepsia*, vol. 43, no. 3, pp. 211–218, 2002.

[12] S. Narasimhan, K. B. Kundassery, K. Gupta, and et al, "Seizure-onset regions demonstrate high inward directed connectivity during resting-state: An seeg study in focal epilepsy," *Epilepsia*, vol. 61, no. 11, pp. 2534–2544, 2020.

[13] D. Hermes and K. J. Miller, "Chapter 19 - ieeg: Dura-lining electrodes," in *Brain-Computer Interfaces* (N. F. Ramsey and J. del R. Milln, eds.), vol. 168 of *Handbook of Clinical Neurology*, pp. 263–277, Elsevier, 2020.